J. Membrane Biol. 147, 7–22 (1995)

The Journal of
Membrane
Biology

Cytoplasmic Ca^{2+} Inhibits the Ryanodine Receptor from Cardiac Muscle

D.R. Laver, L.D. Roden, G.P. Ahern, K.R. Eager, P.R. Junankar, A.F. Dulhunty

Muscle Research Group, Division of Neuroscience, John Curtin School of Medical Research, Australian National University, GPO Box 334, Canberra, ACT 2601, Australia

Received: 30 November 1994/Revised: 24 April 1995

Abstract. Ca^{2+}-dependent inhibition of native and isolated ryanodine receptor (RyR) calcium release channels from sheep heart and rabbit skeletal muscle was investigated using the lipid bilayer technique. We found that cytoplasmic Ca^{2+} inhibited cardiac RyRs with an average K_m = 15 mM, skeletal RyRs with K_m = 0.7 mM and with Hill coefficients of 2 in both isoforms. This is consistent with measurements of Ca^{2+} release from the sarcoplasmic reticulum (SR) in skinned fibers and with [^{3}H]-ryanodine binding to SR vesicles, but is contrary to previous bilayer studies which were unable to demonstrate Ca^{2+}-inhibition in cardiac RyRs (Chu, Fill, Stefani & Entman (1993) J. Membrane Biol. 135, 49–59). Ryanodine prevented Ca^{2+} from inhibiting either cardiac or skeletal RyRs. Ca^{2+}-inhibition in cardiac RyRs appeared to be the most fragile characteristic of channel function, being irreversibly disrupted by 500 mM Cs^+, but not by 500 mM K^+, in the *cis* bath or by solublization with the detergent CHAPS. These treatments had no effect on channel regulation by AMP-PNP, caffeine, ryanodine, ruthenium red, or Ca^{2+}-activation. Ca^{2+}-inhibition in skeletal RyRs was retained in the presence of 500 mM Cs^+. Our results provide an explanation for previous findings in which cardiac RyRs in bilayers with 250 mM Cs^+ in the solutions fail to demonstrate Ca^{2+}-inhibition, while Ca^{2+}-inhibition of Ca^{2+} release is observed in vesicle studies where K^+ is the major cation. A comparison of open and closed probability distributions from individual RyRs suggested that the same gating mechanism mediates Ca^{2+}-inhibition in skeletal RyRs and cardiac RyRs, with different Ca^{2+} affinities for inhibition. We conclude that differences in the Ca^{2+}-inhibition in cardiac and skeletal channels depends on their Ca^{2+} binding properties.

Key words: Ca^{2+}-inhibition — Sarcoplasmic reticulum — Cardiac muscle — Ryanodine receptor — Artificial BLM

Correspondence to: D.R. Laver

Introduction

Excitation-contraction (EC) coupling is the process in muscle which links plasmalemma depolarization to calcium release from the sarcoplasmic reticulum (SR). In both cardiac and skeletal muscle a tissue specific dihydropyridine (DHP) receptor (L-type calcium channel) is the voltage sensor for EC coupling. In cardiac muscle, the influx of Ca^{2+} through DHP receptors is believed to trigger Ca^{2+} release from the SR via ryanodine receptors (RyRs)—the calcium release channels in the terminal cisternae membrane (Nabauer et al., 1989). However, in skeletal muscle DHP receptors are thought to be mechanically coupled to RyRs as Ca^{2+} influx through the DHP receptors is not a prerequisite for muscle contraction (Ashley, Mulligan & Lea, 1991).

The RyR channel is comprised of an unusually large, ~2.3 MDa homotetrameric protein. *In situ,* the skeletal RyR is thought to associate with other proteins including the DHP receptor in the transverse-tubule membrane and with triadin, FK-506 binding protein, calsequestrin, calmodulin, aldolase and glyceraldehyde 3-phosphate dehydrogenase in the junctional gap and SR membrane (Ikemoto et al., 1989; Jayaraman et al., 1992; Brandt et al., 1990; Caswell et al., 1991; Menegazzi et al., 1994; Marty et al., 1994). Though less is known about proteins associated with cardiac RyRs, triadin has been identified in cardiac muscle and FK-506 binding protein and calmodulin-dependent protein kinase are co-isolated with the RyR and may modulate its function (Witcher et al., 1991; Peng et al., 1994; Timerman et al., 1994).

Activation of the RyR from skeletal and cardiac muscle, by micromolar cytoplasmic [Ca^{2+}], has been well established by studies of Ca^{2+} induced Ca^{2+} release (CICR) from SR vesicles containing RyRs, and from

single channel recordings of the RyR in lipid bilayers (Rousseau et al., 1986; Smith, Coronado & Meissner, 1986; Rousseau & Meissner, 1989; Chu et al., 1993). Likewise, cytoplasmic [Ca^{2+}] in the mM range has been shown to inhibit the RyR from skeletal muscle. However, the results obtained for Ca^{2+}-inhibition of the cardiac RyR are conflicting. Measurements of Ca^{2+} release from SR vesicles (Chamberlain, Volpe & Fleischer, 1984; Chu et al., 1993) and skinned cardiac Purkinje cells (Fabiato, 1985), as well as binding of [^{3}H]-ryanodine to SR vesicles (Chu et al., 1993; Fruen et al., 1994) indicate that both cardiac and skeletal isoforms are inhibited by cytoplasmic [Ca^{2+}] above 100 μM, but that the cardiac RyR is at least 10-fold less sensitive to Ca^{2+}-inhibition than its skeletal isoform. In marked contrast, studies of single cardiac RyR channels in lipid bilayers have been unable to demonstrate Ca^{2+}-inhibition of the RyR at concentrations up to 1 mM (Rousseau & Meissner, 1989) and 10 mM (Chu et al., 1993).

This study investigates in depth the Ca^{2+}-dependent inhibition of RyRs from sheep heart and rabbit skeletal muscle in lipid bilayers. The possible effects of the isolation and reconstitution procedures on Ca^{2+}-inhibition of cardiac RyRs in lipid bilayers are examined. Channels incorporated directly from SR vesicles are compared with channels that are first solublized with detergent and incorporated via proteoliposomes. We demonstrate a cytoplasmic Ca^{2+}-dependent inhibition of the cardiac RyR over the range 1–40 mM and explore possible reasons why it has not been reported before in lipid bilayers.

The possibility that similar Ca^{2+}-inhibition gating mechanisms operate in both RyR isoforms was investigated by measuring the probability distributions of RyR channel open and closed durations. The conventional way of testing for similar gating mechanisms is to see if the same kinetic model can describe the gating properties in both channel types. While specific theoretical models are useful for making predictions and directing further research, they are not absolutely necessary for establishing similarity between gating mechanisms. This study uses an alternative method to compare the gating kinetics of different channels. This method is based on standard statistical techniques and does not rely on any specific gating model. The technique determines whether the gating kinetics of two channel types could, in principle, be fitted by the same model. The advantage of this analytical approach is that specific gating models need not be found to explain the data. Furthermore, conclusions based on this analysis are not encumbered by the assumptions attached to specific models.

Materials and Methods

Chemicals and Solutions

Lipids used for planar bilayers were obtained in chloroform from Avanti Polar Lipids (Alabaster, Alabama) and were either stored under nitrogen or in a freezer at −15°C. Lipids were thawed and freshly mixed for each experiment. The lipid mixture was dried under nitrogen and redissolved in n-decane (Aldrich, 99%+) at a concentration of 50 mg/ml. Cesium salts were obtained from Aldrich. $CaCl_2$, sucrose and imidazole were obtained from BDH. Caffeine, KCl and NaCl were obtained from Ajax. TES, CHAPS, EGTA, AMP-PNP, leupeptin, benzamidine, pepstatin A, PMSF and ruthenium red were obtained from Sigma. HEPES and ryanodine were obtained from Calbiochem. Unless otherwise stated, the bathing solutions contained (in mM): CsCl (250 *cis*/50 *trans*), 0.1 or 1 $CaCl_2$, 10 TES (adjusted to pH 7.4 with CsOH). Ca^{2+}-buffered solutions used for perfusing the bath contained (in mM): 250 CsCl, 10 TES and 2 BAPTA. The solutions were adjusted to pH 7.4 with CsOH, and to a range of pCa with $CaCl_2$. Free [Ca^{2+}] was measured using an ion meter (Radiometer ION83). The calibration of the ion meter was routinely checked by comparing its estimates of free [Ca^{2+}] with theoretical estimates derived from the algorithm used by the program COMICS (Perrin & Sayce, 1967) using the standard reaction constants (Tsien, 1980). Addition of AMP-PNP, caffeine, ryanodine, ruthenium red or increasing [Ca^{2+}] to more than 1 mM, was done by adding stock solutions of these substances to the bath while stirring vigorously. Altering [Cs^+] or decreasing [Ca^{2+}] to less than 1 mM was achieved by perfusing the bath with at least four volumes (6 ml) of Ca^{2+}-buffered solution (*see above*) which should produce, at least, a 95% exchange of solutions. Incomplete solution exchange is likely to incur the worst errors when estimating cis [Ca^{2+}]. For example, replacing 95% of a 1 mM Ca^{2+} solution with a 1 μM Ca^{2+} buffer will give a final [Ca^{2+}] of 1.5 μM.

Isolation of SR vesicles

Cardiac SR vesicles were prepared according to Sitsapesan et al. (1991). Unless otherwise stated, buffers contained the protease inhibitors: leupeptin (1 μM), pepstatin A (1 μM), benzamidine (1 mM) and PMSF (0.7 mM). Sheep hearts were excised from anaesthetised ewes (5% pentobartitone (IV) followed by oxygen/halothane) and rinsed in ice cold homogenising buffer (20 mM imidazole, 300 mM sucrose; pH 7.4 with HCl). Ventricular material was stripped of fat and connective tissue, minced and homogenized in a Waring blender, in fresh buffer (4 × 15 sec bursts at high speed, within 15 min of excision). The homogenate was centrifuged at 11,000 *g* for 20 min. The supernatant was then centrifuged at 110,000 *g* for 120 min. The crude vesicle pellet was resuspended in homogenizing buffer containing 10 μM leupeptin and 2 mM DTT, snap frozen and stored in either liquid nitrogen or at −70°C. Some vesicle preparations were fractionated by loading the crude vesicles onto a discontinuous sucrose density gradient consisting of 45%, 38%, 34%, 32%, and 28% sucrose layers w/w (in mM) in 400 KCl, 0.5 $MgCl_2$, 0.5 $CaCl_2$ and 0.5 EGTA, 20 imidazole at pH 7.4 and centrifuged for 16 hr at 100,000 *g* in a Beckman SW28 rotor. Vesicles were collected from the 38%–45% interface, diluted 3-fold in the 400 mM KCl buffer without sucrose (*see above*), pelleted at 125,000 *g* for one hr, resuspended in homogenising buffer with 2 mM DTT (at 10 to 20 mg/ml protein), snap frozen and stored in liquid nitrogen.

SR vesicles from skeletal muscle were prepared according to Chu et al. (1988) using frozen cubes of either back or leg muscle from New Zealand rabbits. Protein concentration was determined by Lowry assay and vesicles were run on SDS-PAGE.

Isolation and Reconstitution of Cardiac RyRs

The method was based on previous reports (Lai et al., 1988; Lindsay & Williams, 1991). Crude SR vesicles (2 mg protein per ml) were resuspended in 25 mM imidazole (pH 7.2) containing L-a-phosphatidylcholine (type XI or XVI, Sigma), (2.5 mg/ml), CHAPS at either

0.5 or 1% (w/v), 1 M NaCl, 0.1 mM EGTA, 0.15 mM $CaCl_2$, 2 mM DTT. The mixture was homogenized using a glass Dounce homogenizer and incubated on ice for one hr. The insoluble material was removed by centrifugation at 100,000 *g* for 45 min before loading the supernatant onto a 5–25% linear sucrose gradient in the above buffer. This was allowed to sediment for 16 hr at 100,000 *g* in a SW28 rotor. Two ml fractions were then collected from the bottom of the centrifuge tubes and aliquots of each fraction were subjected to SDS-PAGE and silver staining in order to identify the fraction containing the high molecular weight protein characteristic of the RyR.

Reconstitution of RyRs into proteoliposomes was achieved by dialyzing fractions containing the RyR against a buffer containing (in mM): 100 NaCl, 0.1 EGTA, 0.15 $CaCl_2$, 25 imidazole, pH 7.2. Dialysis was carried out at 4°C overnight with at least three, 1-l changes of buffer with stirring. Sucrose was added to the proteoliposomes to a final concentration of 200 mM before snap freezing in liquid nitrogen and storing at −70°C.

Artificial Lipid Bilayers and SR Vesicle Fusion

Bilayers were formed from a mixture of PE, PS and PC (5:3:2, by weight) in n-decane (Mueller et al., 1962). The bilayer chamber was a 1.5 ml delrin cup which separated two bathing solutions, called *cis* and *trans*. Bilayers were formed across an aperture of 150 to 200 μm in the wall of the cup. Thinning of the lipid film to a bilayer was monitored visually with 20× magnification and electrically, using measurements of bilayer capacitance. Incorporation of ion channels was achieved as described by Miller & Racker (1976) as follows. SR vesicles were added to a final concentration of 1–10 μg/ml and the bath was stirred vigorously until channel activity indicated vesicle fusion with the bilayer. The side of the bilayer to which the vesicles were added is defined as the *cis* side. Conditions that we found promoted vesicle fussion were (i) a relatively high osmotic potential in the *cis* bath, (ii) mM *cis* $[Ca^{2+}]$ and (iii) vigorous stirring of the *cis* bath. The cytoplasmic side of the SR membrane, when fused with the bilayer, faced the *cis* bath (Miller & Racker, 1976). Stirring of the *cis* and *trans* chambers was done using magnetic stirrers constructed in house. Perfusion of *cis* and *trans* chambers was done with a back-to-back syringe system configured such that bath perfusion and waste withdrawal could be maintained at equal rates. Experiments were carried out at temperatures between 21 and 24°C.

Recording and Analysis of Single Channel Data

Electrical connection with the bath was made using silver chloride coated silver wire immersed in an agar salt-bridge (containing 50 to 250 mM CsCl). Voltage was controlled and current recorded with an Axopatch 200A amplifier (Axon Instruments). Electrical potentials are given with respect to the *trans* chamber as ground and positive current is directed from the *cis* to *trans* bath. During the experiments, the bilayer current and potential were recorded at a bandwidth of 5 or 10 kHz on videotape using pulse code modulation (Model 200; A.R. Vetter).

The current signals were replayed and digitized with a TL-1 DMA interface (Tecmar) prior to analysis. For measurements of unitary current, I, and open probability, P_o, the current signal was passed through a 1 kHz, low pass, 8-pole Bessel filter and sampled at 2 kHz. Unitary current was determined from the separation of the peaks in the amplitude distributions which correspond to the open and closed events. P_o was calculated from the time-average current within bursts divided by the unitary current. Bursts are defined as periods of gating activity terminated by closed level durations in excess of 1 sec. This burst threshold was decided on the basis of the closed time frequency distributions which showed that for cytoplasmic $[Ca^{2+}] > 1$ μM nearly all the closed durations were associated with exponential decay constants shorter than 0.1 sec. Unitary current and time-averaged currents were measured using an in-house program (Channel 2, developed by Professor P.W. Gage and Mr. M. Smith).

The gating kinetics were quantified by the probability distributions of open and closed durations obtained from single-channel recordings with stationary kinetics. Gating kinetics were considered to be stationary if values of P_o determined from 1-sec segments of bursts (*defined above*) varied by less than 20%. Open and closed durations were extracted from current records using the Hidden Markov Model (HMM, the details of this program are given by Chung et al., 1990). HMM, as implemented here, determines the most likely channel gating sequence, assuming that the data are composed of a *two-level* Markov signal, embedded in white, Gaussian noise. For HMM analysis, the current signal was replayed at a bandwidth of 5 kHz and digitized at either 10 kHz or 50 kHz. The 10 kHz sampling rate is the bare minimum (the Nyquist frequency) and a more accurate rendition of the signal can be achieved with the higher sampling rate. However, Chung et al. (1990) point out that over-sampling data introduces short-term memory into the signal which violates the assumption of white noise. This blurs the distinction between the Markov signal and the noise and so results in a higher probability of errors in the calculated signal sequence. As yet no systematic study of this problem has been published. Therefore, in order to see how our results depended on the sampling rate we analyzed several single channel recordings which had been digitized at both low and high rates.

Frequency distributions of open and closed durations were presented using variable bin widths with equal separation on a log scale as described by Sigworth & Sine (1987). This data representation provided a uniform statistical weighing of the data across the entire range of durations and the exponential components within these distributions could be easily discerned as peaks in the data (e.g., *see* Fig. 11).

Abbreviations

AMP-PNP	5-adenylylimododiphosphate
ATP	adenosine-5′triphosphate
BAPTA	1,2-bis(2-aminophenoxy)ethane-NNN′N′-tetraacetic acid
CHAPS	3-[(3-cholamidopropyl) dimethylammonio]-2-hydroxy-1-propanesulfonate
DTT	dithiothreitol
EGTA	[ethylene bis (oxyethylenenotrilo)] tetraacetic acid
PC	palmitoyl-oleoyl-phosphatidylcholine
PE	palmitoyl-oleoyl-phosphatidylethanolamine
PS	palmitoyl-oleoyl-phosphatidylserine
PMSF	phenylmethylsulfonyfluoride
SDS-PAGE	sodium dodecyl sulfate-polyacrylamide gel electrophoresis
TES	N-tri[Hydroxymethyl] methyl-2-aminoethanesulfonic acid

Results

Fusion of SR Vesicles with Lipid Bilayers

Artificial planar bilayers were stable for several hours and had capacitances in the range 200–300 pF and conductances of less than 10 pS. The electrical noise on the bilayer current was 5 pA (RMS) at a bandwidth of 5 kHz

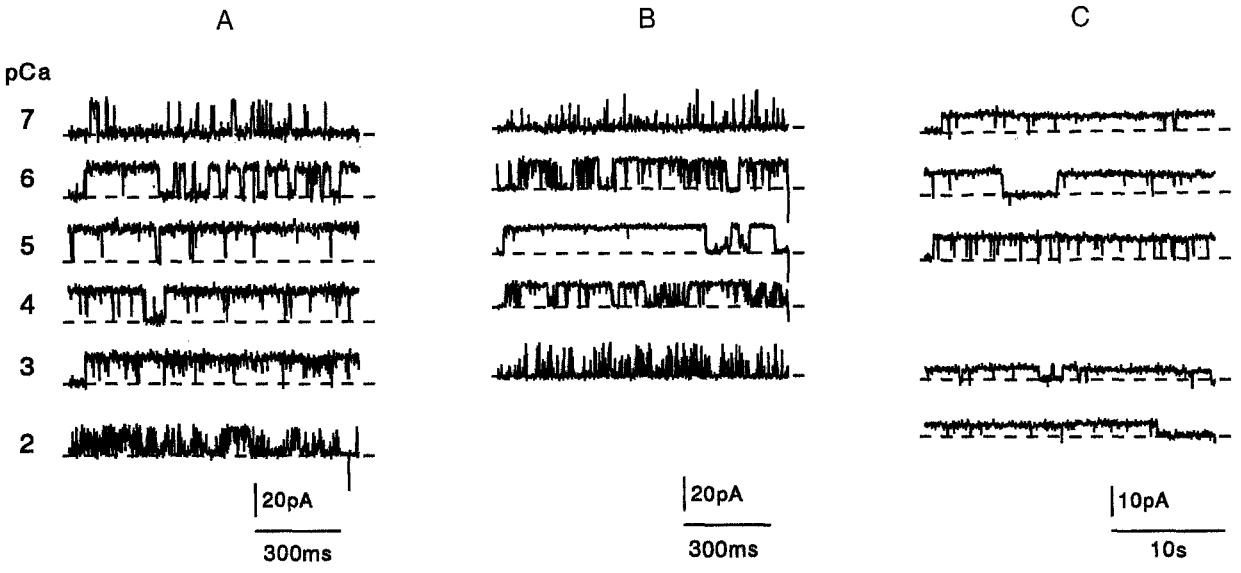

Fig. 1. Short representative segments of current recordings from single RyRs in planar lipid bilayers showing the effects of cytoplasmic [Ca^{2+}] and ryanodine on channel gating with 250 mM/50 mM CsCl (*cis/trans*). The bilayer potential is +40 mV (*trans* or lumen side at ground) and channel openings are shown as upward current transitions from the baseline (broken line). (*A*) RyR channel from cardiac muscle. (*B*) RyR from skeletal muscle. (*C*) RyR channel from cardiac muscle in the presence of 30 μM ryanodine in the *cis* (cytoplasmic) bath. Ca^{2+}-activation in both channel types is similar, but Ca^{2+}-inhibition occurs at much lower concentrations in RyR from skeletal muscle than from cardiac muscle. Ryanodine reduces channel conductance and causes the channel to remain open over the entire experimental range of *cis* [Ca^{2+}]. pCa for each trace is shown at the extreme left.

and its power spectral density was proportional to frequency over the range 1–5 kHz.

The rate of fusion of cardiac SR vesicles with lipid bilayers depended on the composition of the solution in the *cis* bath. In the presence of the standard 250 mM CsCl solution, vesicle fusion occurred with an 80% probability within 10 min of their addition to the *cis* chamber (n = 133). Several types of channels were observed from cardiac SR vesicles under these conditions. Incorporations of Cl^- channels, similar to those reported by Rousseau (1989) were most frequently observed (85% of fusions) and RyRs were observed in 27% of fusions. Incorporation of RyR channels without Cl^- channels occurred in only 14% of cases. These statistics showed no significant variation between different vesicle preparations. In one instance, a channel with mitochondrial VDAC properties was incorporated. VDAC channels were more frequently seen when proteins had been solublized with the detergent, CHAPS, before incorporation into lipid bilayers. When the *cis* bath contained 500 mM CsCl the vesicle fusion rate was double that in 250 mM CsCl (n = 35), and the proportion of fusions which introduced RyRs into the bilayer was much larger. RyRs were observed in 80% of fusions and Cl^- channels were seen in 20% of vesicle fusions in 500 mM CsCl. We found that bilayer stability was noticeably reduced after incorporation of SR vesicles and that potential differences (V_m) larger than ±80 mV were likely to rupture the bilayer. Only 15% of bilayers lasted for more than 10 min after RyRs were first recorded. However, incorporation of proteoliposomes did not destabilize the lipid bilayers.

Characterizing the Ryanodine Receptor Calcium Release Channel in Lipid Bilayers

The RyR calcium channels from skeletal and cardiac muscle could be unambiguously identified by their well-known ion permeation and ligand binding properties as follows. Ryanodine (30 μM in the *cis* bath) "locked" the channels into an open state, with a reduced conductance. The gating kinetics of the ryanodine-affected channel were also much slower and were insensitive to channel modulators (Fig. 1*C*). The channels were activated by μM cytoplasmic (*cis*) Ca^{2+} (Fig. 1*A* and *B*) and mM concentrations of caffeine and AMP–PNP, a nonhydrolyzable analogue of ATP (*data not shown*). The channels were inhibited by 1 mM *cis* Mg^{2+} in the presence of 10 μM Ca^{2+} and by ruthenium red (15 μM) (*data not shown*). The modulation of the cardiac RyRs by these compounds was the same as that found by others (Rousseau et al., 1986; Rousseau, Smith & Meissner, 1987; Sitsapesan & Williams, 1990; Ashley & Williams, 1990).

The conductance of the cardiac RyR in symmetric 250 mM CsCl was 525 ± 10 pS, which is close to the 517 pS interpolated from the [Cs^+]-dependence of RyR conductance reported by Tinker, Lindsay & Williams

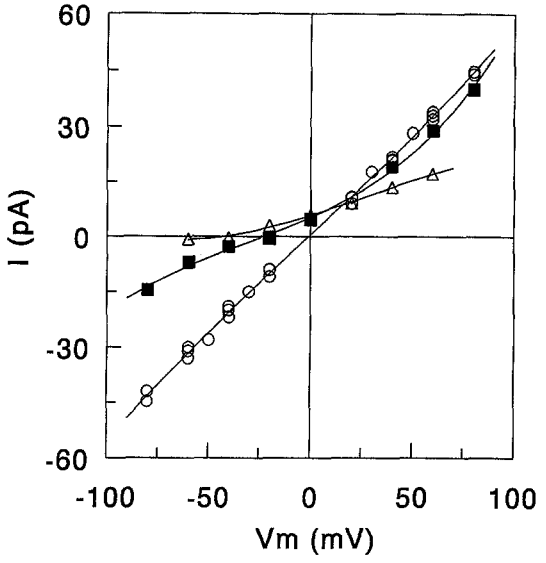

Fig. 2. Current-voltage characteristics of cardiac RyR channels in: (○)—symmetric solutions containing 250 mM CsCl and free-[Ca^{2+}] less than 100 μM (conductance at 0 mV = 525 pS); (■)—*cis* 250 mM CsCl + 1 mM $CaCl_2$, *trans* 50 mM CsCl + 1 mM $CaCl_2$ (reversal potential = −23 ± 4 mV); (△)-*cis* 250 mM CsCl + 40 mM $CaCl_2$, *trans* 50 CsCl + 1 mM $CaCl_2$ (reversal potential = −43 ± 6 mV). The solid lines are third order, polynomial fits to the data used to calculate the reversal potentials.

(1992). With Cs^+ as the main current carrier the RyR channel conductance and current reversal potentials were sensitive to mM [Ca^{2+}] in both the *cis* (Fig. 2) and *trans* (*data not shown*) chambers. The relative permeability of Ca^{2+} with respect to Cs^+(P_{Ca}/P_{Cs}) derived from the current reversal potentials was found to lie in the range 13 to 30. This approximate result is similar to the value of 11 from earlier, more precise studies of ion permeability (P_{Ca}/P_{Cs} is calculated from the product of the RyR permeability ratios: P_{Ca}/P_K from Lindsay & Williams (1991) and P_K/P_{Cs} from Lindsay, Manning & Williams (1991)).

General Observations of RyR Channel Gating; Voltage and [Ca^{2+}]-dependence

The gating kinetics of cardiac RyRs were found to differ between individual channels. While most channels (>95%) incorporated from SR vesicles exhibited stationary gating properties, some channels underwent abrupt changes in gating behavior, or mode switching, several times per minute (e.g., *see* Fig. 3 *A* and *B*). Similar mode switching behavior in RyRs from skeletal and cardiac muscle has been shown in other studies (eg., Smith et al., 1986; Ashley & Williams, 1990; Chu et al., 1993; Zahradnikova & Palade, 1993). The properties of cardiac RyRs were measured from 7 crude vesicle preparations and from one preparation which had been further fractionated on a sucrose gradient (*see* Materials and Methods). There was no correlation between RyR kinetics and the vesicle preparations. We also found that removing PS from the bilayer forming lipid mixture had no effect on Ca^{2+}-dependent gating of RyRs.

The activity of cardiac RyRs commonly ceased after a period when the V_m was stepped to positive values. This period varied between channels, from several seconds to minutes. Channels could be reactivated by negative voltage pulses lasting several seconds. This voltage-dependent "inactivation" was also present in channels modified by ryanodine (Fig. 3*D*).[1] In contrast to the inactivation, the voltage-dependence of channel open probability *within bursts*, P_o, (*see* Materials and Methods) was such that the channel was more open at positive bilayer potentials (Fig. 4). Similar voltage-dependencies have been reported elsewhere for inactivation (Rousseau et al., 1986) and P_o within bursts (Rousseau & Meissner, 1989). Frequency histograms of P_o at 10 μM and 1 mM cytoplasmic [Ca^{2+}] both reveal a broad distribution (Fig. 5), which reflected the wide variability of the channel gating properties.

Histograms of cardiac RyR channel current amplitudes (Fig. 6*A*) show that, for a variety of gating modes, gating consists mainly of transitions between two conducting states, namely fully open and closed. On occasion, the channel would switch into a "substate mode" for several seconds in which gating was dominated by current transitions between what appeared to be many, poorly resolved subconductance states (Fig. 6*B*). Substate modes constituted less than 5% of the channel activity and these sections of data were not included in any detailed analysis of channel gating.

The gating patterns of RyRs from both skeletal and cardiac muscle were examined over a wide range of cytosolic (*cis*) [Ca^{2+}]. The dependence of the mean P_o within bursts on *cis* [Ca^{2+}] is shown in Fig. 7*A*. Examples of single channel recordings from which these data was derived are shown in Fig. 1 (*see above*). Activation of RyRs by [Ca^{2+}] occurred in the range 0.1 μM to 10 μM. Ca^{2+}-activation was observed in all channels and exhibited characteristics similar to those observed in other bilayer studies (*see below*). The [Ca^{2+}]-dependence of P_o within bursts followed the same trend as the mean current from whole recordings. However, the latter results showed additional variation arising from the inclusion of a relatively few long closed periods.

Channel activation and inhibition were characterized by fitting the Ca^{2+}-dependence of P_o with the dose response function given by Eq.1

[1] These results have been confirmed in a recent study by Ma (1995).

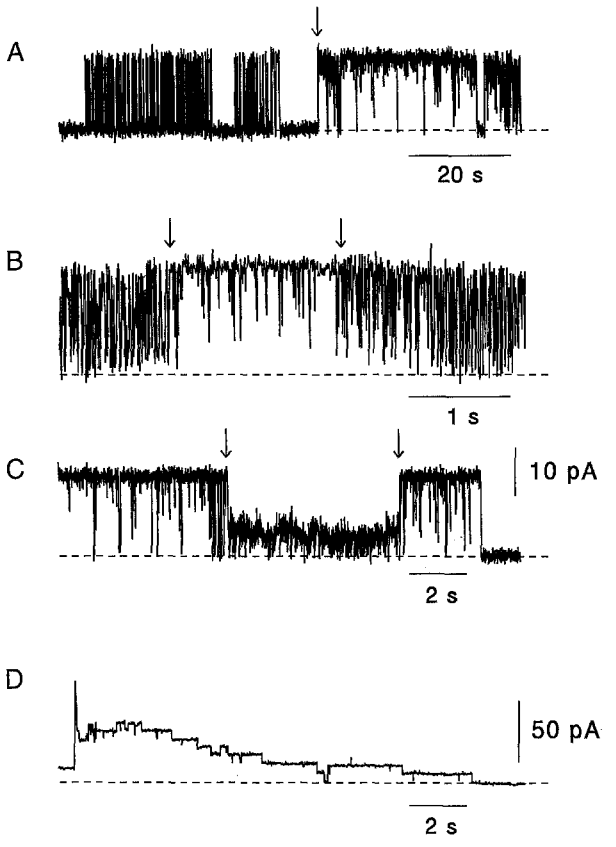

Fig. 3. Segments of current recordings from cardiac RyR channels incorporated into planar lipid bilayers from SR vesicles. The records show several nonstationary aspects of RyR gating kinetics. The bilayer potential is +40 mV and channel openings are shown as upward current transitions from the baseline (broken line). The 10 pA scale bar applies to records *A-C*. (*A*) shows two RyR channels in the same bilayer with different gating kinetics. The activity of one gives way to the other at approximately halfway through the segment (arrow). The later superposition of both channel signals (*not shown*) indicated that two separate channels generated this current (*B*) shows a transient change (between the arrows) in the gating pattern of an individual RyR in which P_o changes from about 0.6 to about 0.95 (*C*) shows another transient change in the gating mode in which the channel conductance enters a "substate" mode — indicated between the arrows (*D*) shows how the activity of 7 RyRs decays after a step change in voltage from −40 mV to +40 mV. The channels are relatively active at −40 mV. Though voltage-dependent inactivation occurs in native RyRs, ryanodine (30 μM) modified RyRs are shown in *D* because their slower gating kinetics allows this inactivation process to be clearly seen.

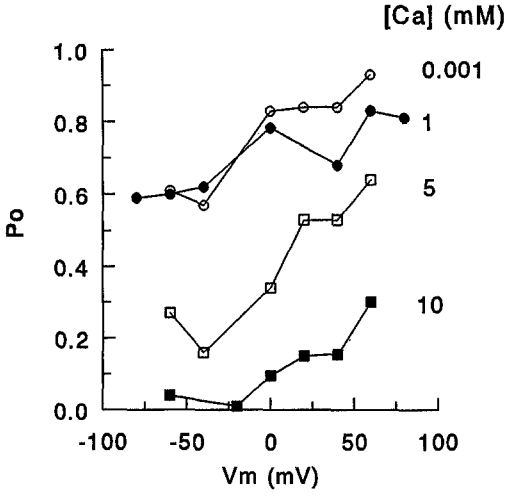

Fig. 4. The voltage-dependence of cardiac RyR open probability, P_o, at various $[Ca^{2+}]$ in the *cis* bath. Bilayers were bathed in 250 mM/50 mM CsCl (*cis/trans*) (*see* Materials and Methods)

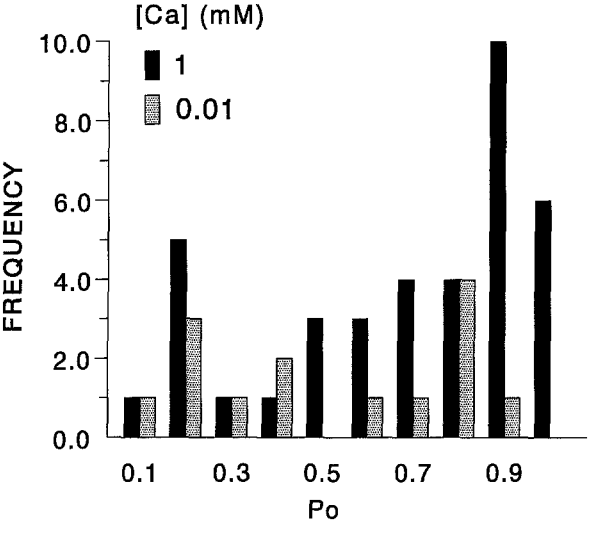

Fig. 5. Frequency distributions of cardiac RyR open probabilities obtained from 45 measurements of channels in 29 bilayers bathed in 250 mM/50 mM CsCl (*cis/trans*), also containing either *cis* 10 μM or 1 mM Ca^{2+} at a bilayer PD of +40 mV. The large spread in P_o is indicative of large variations in the gating kinetics of different channels under identical experimental conditions.

$$P_o = P_m \left(\frac{1}{1 + (K_A/[Ca^{2+}])^{H_A}} \right) \times \left(1 - \left(\frac{1}{1 + (K_I/[Ca^{2+}])^{H_I}} \right) \right) \quad (1)$$

where P_m is the open probability of the fully activated channel, K_A and K_I are the binding affinities of the activation and inhibition respectively and H_A and H_I are the Hill coefficients of activation and inhibition respectively. The Hill coefficients represent the number of Ca^{2+} which bind cooperatively to produce either channel activation or inhibition. The activation characteristics of cardiac and skeletal RyRs are similar and are also in agreement with the mean Ca^{2+}-activation characteristics reported in other studies. For the cardiac RyR channel P_m = 0.55, K_A = 1 μM and H_A = 1 (Chu et al., 1993, K_A = 1 μM and H_A = 1.1; Rousseau & Meissner, 1989, K_A = 0.7 μM and

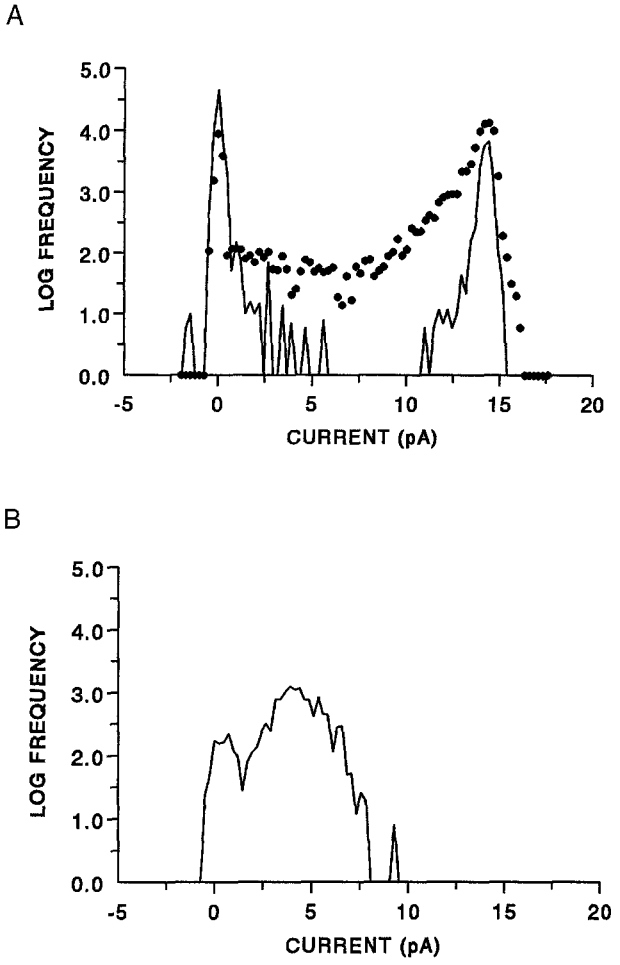

Fig. 6. Histograms of channel amplitudes compiled from single-channel recordings. (*A*) Frequency distribution of event amplitudes which only include events long enough to be accurately determined (>2.5 msec). These were compiled from the data shown in Fig. 3 as follows: (line)-first segment of Fig. 3*A* before the arrow. (●) second segment of Fig. 3*A* after the arrow (*B*) the RyR substate mode shown in Fig. 3*C* between the arrows.

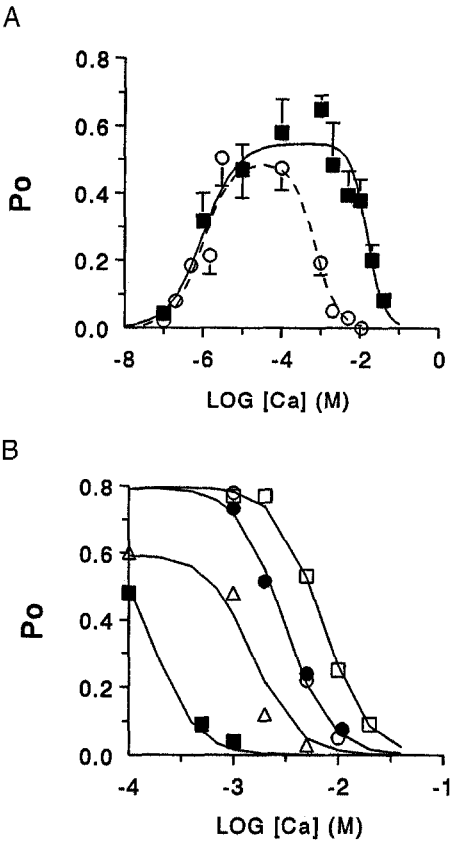

Fig. 7. The dependence of channel open probability, P_o, on cytosolic (*cis*) [Ca^{2+}], in solutions containing 250 mM/50 mM CsCl (*cis/trans*), for; (*A*) RyRs from sheep heart (■, mean of = 32 RyRs) and rabbit skeletal muscle (○, mean of 33 RyRs). The lines show the solutions to Eq. 1 for the following parameter values: (continuous line) $P_m = 0.55$, $H_A = 1$, $K_A = 1$ μM, $H_I = 1.7$, $K_I = 15$ mM. (broken line) $P_m = 0.5$, $H_A = 1$, $K_A = 1$ μM, $H_I = 1.5$, $K_I = 700$ μM. (*B*) several individual RyR. The lines show solutions to Eq. 1 for $H_I = 2$. The values for K_I associated with the data from cardiac muscle are:- (□)- 7 mM; (○)- 3 mM; (△)- 1.5 mM; and skeletal muscle are:- (●)- 3 mM; (■)- 0.16 mM. These data illustrate the size of the variations that can occur between the Ca^{2+}-inhibition properties of different channels.

H_A = 1.3). Likewise, for skeletal RyR channels, P_m = 0.5, K_A = 1 μM and H_A = 1.2 (Chu et al., 1993, K_A = *1* μM and H_A = 1.2). However, recent measurements of Ca^{2+}-activation in *individual* RyRs from sheep heart, produced Hill coefficients ranging from 2 to 4 (Sitsapesan & Williams, 1994). Sitsapesan & Williams (1994) believed that their relatively high Hill coefficients resulted from an improvement in the signal-to-noise ratio of their single channel recordings over earlier studies which used Ca^{2+} as the permeant ion. However, our lower estimates of Hill coefficient are also obtained from high resolution channel recordings. It is more likely then, given the variations in the Ca^{2+} -activation characteristics of RyRs, that the lower Hill coefficients observed here and by others (*see above*) may be due to the averaging of the results from several channels with varying Ca^{2+} sensitivities (*see below*).

Cardiac RyRs solublized with CHAPS were activated at similar Ca^{2+} concentrations as the native channels. Though they had the same, main-state Cs^+ conductance as native RyRs, they had longer substate levels at ~25 and ~75% of their maximum conductance. Also, mode switching behavior was more frequently observed in solublized RyR channels (30% of channels).

Inhibition of Cardiac and Skeletal RyRs by *cis* Calcium

Both cardiac and skeletal RyRs were inhibited by mM concentrations of *cis* Ca^{2+}. Calcium-dependent inhibition of skeletal RyRs from SR vesicles occurred in all instances (n = 7) when *cis* [Ca^{2+}] was increased above

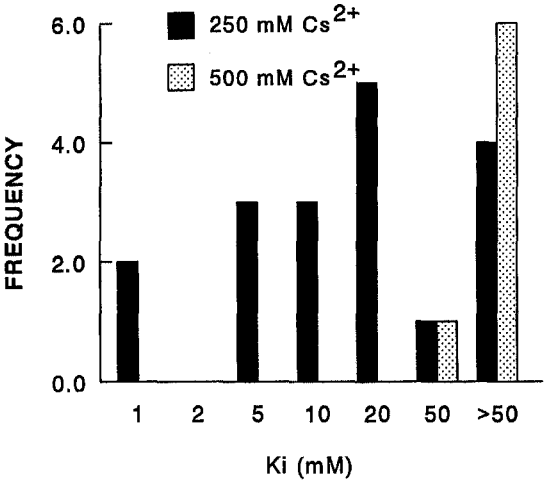

Fig. 8. The frequency distribution of Ca^{2+}-binding affinity for inhibition, K_I, of the cardiac RyR. K_Is were derived from a fit of Eq. 1 to the Ca^{2+}-dependence of P_o. Fits were obtained for data from 14 RyRs with *cis* [Cs^+] of either 250 or 500 mM.

100 μM in the presence of 250 mM Cs^+ (*see* Figs. 1 and 7). The RyR from cardiac SR vesicles was, on average, 20-fold less sensitive to *cis* [Ca^{2+}]; generally showing inhibition when *cis* [Ca^{2+}] exceeded 1 mM (17 out of 21 observations; Figs. 1 and 7). The Ca^{2+}-inhibition process was characterized by measurements of P_o within bursts and in a later section from probability distributions of channel open and closed durations.

Fitting the mean values of P_o shown in Fig. 7*A* with Eq. 1 gave values of $K_I = 0.7$ and 15 mM and $H_I = 1.5$ and 1.7, for skeletal and cardiac RyRs respectively. The values obtained for the skeletal RyRs were consistent with those found previously in bilayer studies (Chu et al., 1993, $K_I = 400$ μM and $H_I = 1.2$). The Ca^{2+} sensitivity of cardiac RyR inhibition was similar to the Ca^{2+}-inhibition of [^{3}H]-ryanodine binding to cardiac SR (K_I = 5–10 mM, Pessah, Waterhouse & Casida, 1985; Chu et al., 1993; Fruen et al., 1994), but was lower than that for CICR from SR vesicles (K_I = 10 μM–1 mM, Chamberlain et al., 1984; Zimanyi & Pessah, 1991; Chu et al., 1993). Ca^{2+}-inhibition of channel gating has not been reported in previous bilayer studies.

The Ca^{2+}-dependence of P_o for individual channels (Fig. 7*B*) revealed kinetics for Ca^{2+}-inhibition which differed from those determined for the mean values of P_o (Fig. 7*A*). The Hill coefficients determined from 4 individual cardiac and 3 individual skeletal RyRs were found to be 2, which is higher than the values of 1.7 (cardiac RyRs) and 1.5 (skeletal RyRs) obtained from the mean data. This difference is a consequence of the large variation in the Ca^{2+}-sensitivities for channel inhibition between bilayers. The variation is illustrated in Fig. 8 where 60% of measurements of K_I for the cardiac RyRs varied between 5 and 20 mM (n = 20). Consequently, averaging the data from several recordings tends to smear out the Ca^{2+}-dependence and reduce the apparent Hill coefficient. Skeletal RyRs also showed considerable variation in K_I. There was no correlation between K_I and different SR vesicle preparations.

The Effect of RyR Solublization Using the Detergent CHAPS on Ca^{2+}-inhibition

Ca^{2+}-dependent inhibition of cardiac RyRs was not observed in four out of six channels after CHAPS solublization, and reconstitution in proteoliposomes. These channels retained their normal response to AMP-PNP, ryanodine, and activation by Ca^{2+}. An abbreviated isolation protocol in which the separation of RyRs on a sucrose gradient was omitted, also yielded channels that were insensitive to Ca^{2+}-inhibition. The Ca^{2+}-dependence of P_o measured from solublized RyRs are compared with that for native RyRs in Fig. 9*A*.

The Effects of High *cis* [Cs^+] on Ca^{2+}-inhibition

Fusion of SR vesicles with lipid bilayers in the presence of 500 mM CsCl in the *cis* bath also introduced RyRs which lacked Ca^{2+}-inhibition. These channels retained their normal response to other ligands, namely caffeine, AMP-PNP, ryanodine, ruthenium red and activation by Ca^{2+}. The Ca^{2+}-dependence of P_o of cardiac and skeletal RyRs in the presence of 500 mM and 250 mM CsCl are compared in Fig. 9. Eighty percent of channels showed Ca^{2+}-inhibition when incorporated into the bilayer with 250 mM *cis* CsCl, compared with only 10% of channels incorporated with 500 mM *cis* CsCl (Figs. 8 and 9*A*). The presence of 500 mM K^+ in the bath did not affect Ca^{2+}-inhibition, nor did fractionating cardiac SR vesicles in the presence of 400 mM K^+ (*see* Materials and Methods). Thus it appears that Cs^+ is more effective than K^+ and Cl^- at disrupting Ca^{2+}-inhibition in cardiac RyRs. In skeletal RyRs there was no significant difference in their Ca^{2+}-inhibition in either 250 mM *cis* [Cs^+] (n = 4) or 500 mM *cis* [Cs^+] (n = 8, *see* Fig. 9*B*).

We conducted two types of experiments in which *cis* [Cs^+] was altered after fusion of RyRs with the bilayer. In the first type of experiment, vesicles were incorporated in 500 mM Cs^+ and then the [Cs^+] was lowered to 250 mM. Ca^{2+} inhibition was not restored within 5 min of reducing the *cis* [Cs^+] (n = 4), showing that the effect of high [Cs^+] on Ca^{2+}-inhibition was irreversible. Secondly, RyRs were incorporated in the presence of 250 mM Cs^+ and 1 mM Ca^{2+}, the *cis* [Cs^+] was increased by perfusing with 500 mM CsCl and then $CaCl_2$ added to 20 mM to inhibit the channel. Channel activity (i.e., P_o, n =

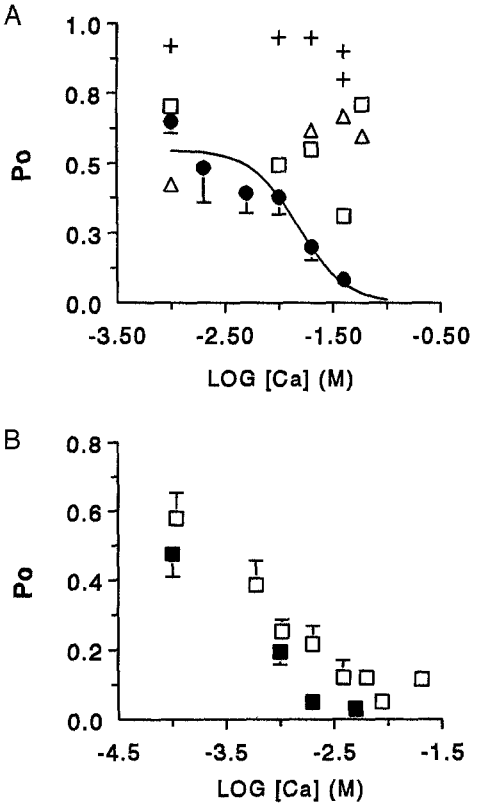

Fig. 9. The fragility of the Ca^{2+}-inhibition in the cardiac RyR. These data show that Ca^{2+}-inhibition can be disrupted by either using CHAPS (1%) to solublize the protein or by exposing RyRs in bilayers to 500 mM Cs^+. The Ca^{2+}-dependence of P_o for; (*A*) cardiac RyRs incorporated into bilayers from:- (●)- SR vesicles in the presence of 250 mM/50 mM Cs^+ (*cis/trans*); (△)-SR vesicles in the presence of 500 mM/50 mM CsCl (*cis/trans*); (+)- SR vesicles in the presence of ryanodine (30 μM *cis*); (□)- liposomes containing RyR solublized using CHAPS in the presence of 250 mM/50 mM CsCl. (*cis/trans*) (*B*) skeletal RyRs in either 250 mM *cis* [CsCl] (■) or 500 mM *cis* [CsCl] (□).

3) increased gradually over several minutes, indicating a gradual loss of Ca^{2+}-inhibition (Fig. 10).

Ryanodine Removes Ca^{2+}-dependent inhibition

Ryanodine (30 μM *cis*) radically altered the gating and conductance properties of RyRs from skeletal and cardiac muscle (Fig. 1*C*, *above*). Ryanodine modification of RyRs was carried out under conditions where P_o was relatively high because it is generally recognized that ryanodine only binds to open channels. The $[Ca^{2+}]$-dependence of channel opening was then measured by perfusing the *cis* bath with ryanodine-free, Ca^{2+}-buffered solutions. As found by others (e.g., Rousseau, Smith & Meissner, 1987), the ryanodine effect was irreversible and gating kinetics of the ryanodine modified channel were insensitive to Ca^{2+}-dependent activation. In addition, we found that ryanodine removed Ca^{2+}-dependent inhibition. Thus P_o, for ryanodine-modified channels, was independent of *cis* $[Ca^{2+}]$ over the range 1 nM to 40 mM (*see* Fig. 9*A*). This is consistent with the effects of ryanodine on CICR from skeletal muscle SR vesicles in high cytoplasmic $[Ca^{2+}]$ (Meissner, 1986).

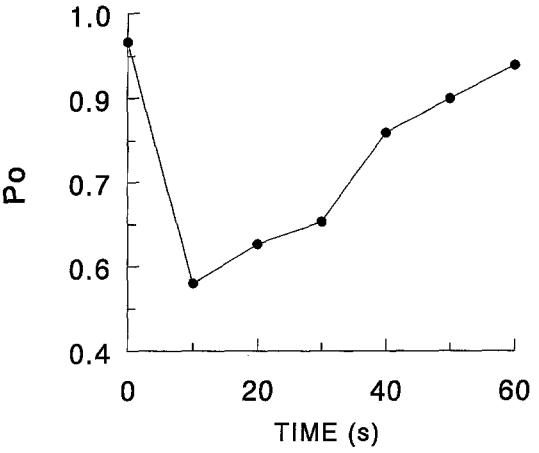

Fig. 10. The time course of the open probability of a cardiac RyR after exposure to 500 mM Cs^+. The channel was incorporated with the bilayer in the presence of 250 mM/50 mM Cs^+ (*cis/trans*). The *cis* bath was replaced by perfusion with a solution containing 500 mM CsCl, immediately followed by the addition of 20 mM $CaCl_2$ (time = 0). P_o then decreased due to Ca^{2+}-dependent inhibition of the channel. The subsequent rise in P_o presumably indicates a gradual removal of channel inhibition.

Probability Distributions of Open and Closed Durations during Ca^{2+}-Inhibition

Probability distributions of event durations were produced by normalizing their frequency histograms. At sub-inhibiting *cis* $[Ca^{2+}]$, the probability distributions of cardiac RyR closed (Fig. 11*A*) and open durations (Fig. 11*C*) were each well described by the sum of three exponentials, as reported by previous investigators (Ashley & Williams, 1990; Chu et al., 1993). We found significant variation in the probability distributions obtained from one RyR to another, reflecting the variations observed in their gating patterns (e.g., Fig. 3*A*, *above*). However, Ca^{2+}-inhibited cardiac RyRs all had similar gating kinetics regardless of their Ca^{2+}-sensitivity. Ca^{2+}-inhibition produced shorter open durations (Fig. 11*D*) and longer closed durations (Fig. 11*B*). In general, when two RyRs with different Ca^{2+}-sensitivities had similar gating patterns at subinhibiting $[Ca^{2+}]$ then, at the same degree of Ca^{2+}-inhibition (i.e., % reduction in P_o), their gating patterns were also similar. This is shown in Fig. 11 where the probability distributions of open and closed times for two cardiac RyRs with high and low Ca^{2+}-sensitivity are compared. By a fortuitous choice of *cis* $[Ca^{2+}]$, both channels had the same values of P_o at subinhibiting (Fig. 11*A* & *C*) and inhibiting $[Ca^{2+}]$ (Fig. 11*B* & *D*). The probability distributions for both channels are nearly identical. Fig. 11*E* & *F* show the probability distributions obtained from the same records as in Fig. 11*A* & *C* except that the data in Fig. 11*E* & *F* was

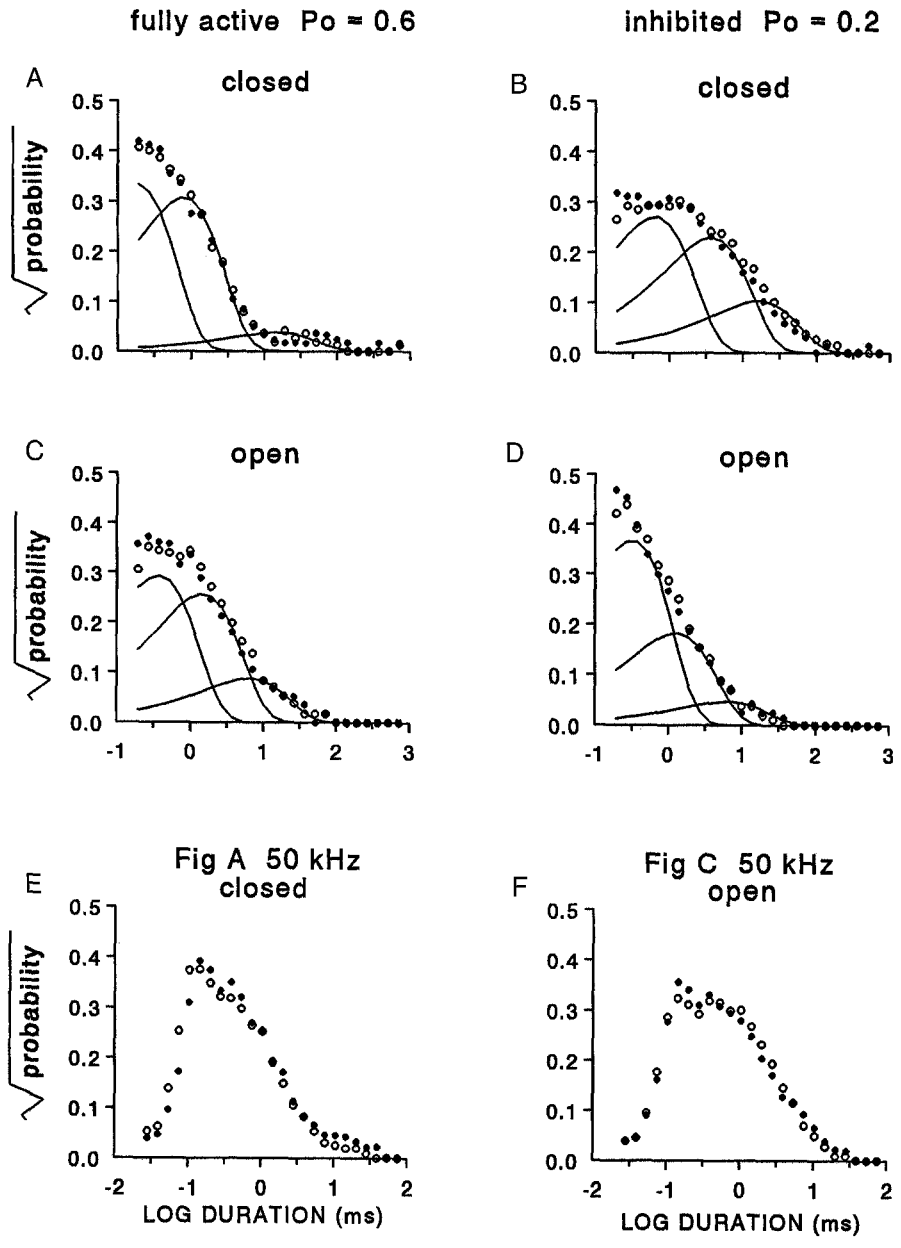

Fig. 11. The square root of the probability of open and closed events of a specific duration verses their duration derived from normalized frequency histograms. The frequency histograms were compiled from data sampled at either 10 kHz (*A-D*) or 50 kHz (*E,F*). Graphs *A-D* compare the probability distributions of closed (*A,B*) and open (*C,D*) durations for two cardiac RyRs with very different sensitivities to inhibition by Ca^{2+}. One channel shows a binding affinity for Ca^{2+}-inhibition, K_I = 7 mM (○) and for the other K_I = 2 mM (●). These are shown (*A,C*) at sub-inhibiting *cis* [Ca^{2+}], (●-1 mM and ○-5 mM) and (*B,D*) *cis* [Ca^{2+}] which produced significant inhibition (●-10 mM and ○-40 mM). Graphs *E* and *F* show the probability distributions obtained from the same records used for Graphs *A* and *C* except that the data were sampled at 50 kHz. The shortest detectable events (dead time) is ~100 μsec. Digitizing the data at higher rates seems to increase the probability of detecting events shorter than ~200 μsec. Frequency distributions of open and closed times were determined using signal analysis program HMM (Chung et al., 1990). The data are presented using the log-bin scaling of frequency distributions devised by Sigworth & Sine (1987). In addition, each data set is normalized by the total number of events in the record to allow a direct comparison of data points. The resulting probability distributions can be adequately fitted by the sum of at least three exponential components (lines). This scaling shows the exponential components as peaks located at ordinates equal to the time constant of the exponential. The gating of both channels is affected in exactly the same way by increasing *cis* [Ca^{2+}].

sampled at five times the rate (50 kHz). The increased sampling rate appears to improve the detectability of the shortest events as seen by a slight increase in their probability. Though, more importantly, the kinetics of the two channels are indistinguishable regardless of the data sampling rate.

There was a surprisingly tight relationship between the gating (i.e., the distribution of open and closed times)

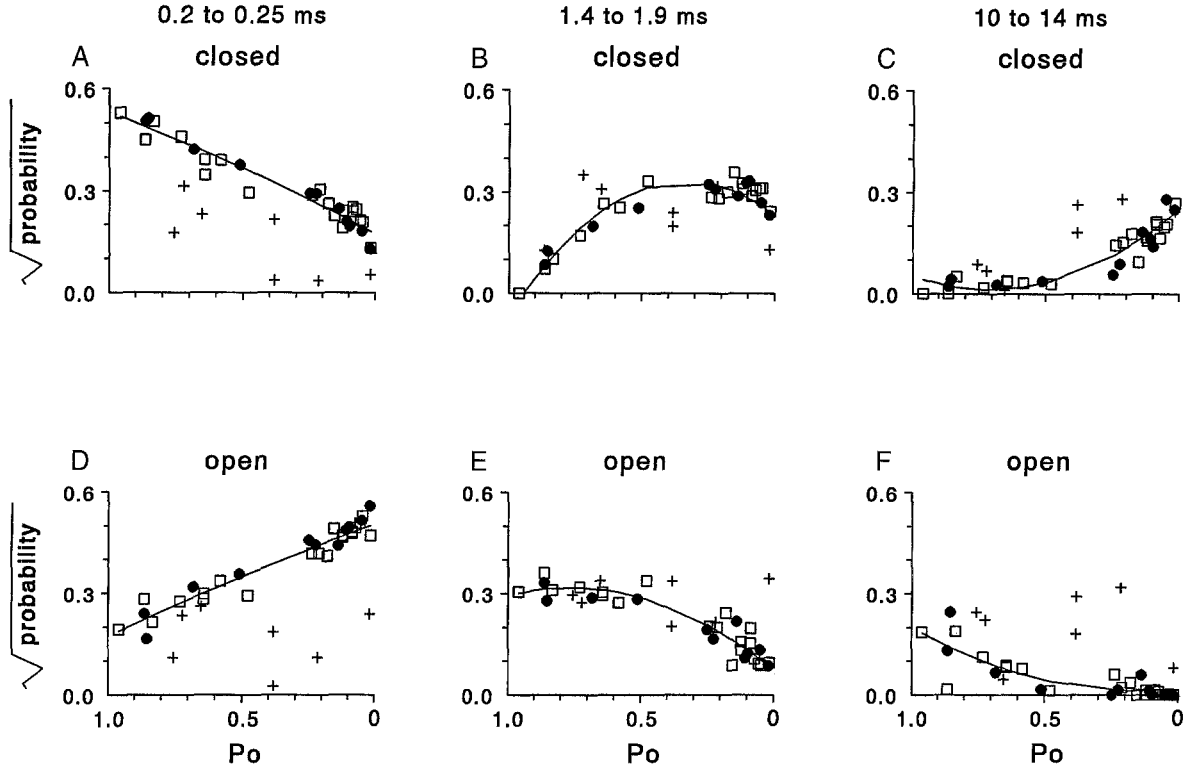

Fig. 12. The effect of Ca^{2+}-inhibition on the gating of several RyRs. The square root of the probability of open and closed events with three specific durations is plotted against the mean open probability for each RyR. The probabilities were derived from data digitized at 10 kHz. The probabilities for closed (*A-C*) and open events (*D-F*) are taken from three histogram bins representing short (*A,D*), medium (*B,E*) and long (*C,F*) durations in the histograms of 8 cardiac (□) and 4 skeletal RyRs (●) at various degrees of Ca^{2+}-inhibition (i.e., P_o). Data with low P_o are from RyRs which are inhibited by high *cis* [Ca^{2+}]. The reasons for comparing gating kinetics by their associated value of P_o rather than experimental *cis* [Ca^{2+}] are given in the text. The solid lines show the quadratic fits to the data used for adjusting nearby data points with small differences in P_o (*see* Analysis of probability distributions of event durations). The probabilities of the three event durations in all the cardiac and skeletal RyRs appear to follow the same trends. This was the case for all 30 data bins in both open and closed histograms. The crosses (+) show duration-probabilities for cardiac RyRs at activating (i.e., μM) *cis* [Ca^{2+}]. The different trends for Ca^{2+}-activation and Ca^{2+}-inhibition suggest that different gating patterns are associated with Ca^{2+}-activation and inhibition.

and the degree of channel inhibition (indicated by P_o) at mM [Ca^{2+}], when individual cardiac RyRs were compared and when cardiac and skeletal RyRs were compared. This is shown in Fig. 12, where the relative occurrence of events of specified duration (the square root of their probability) is plotted against P_o. At subinhibiting *cis* [Ca^{2+}] when P_o was high, closures were dominated by brief events (0.2 msec) and openings were evenly distributed over the three time intervals considered (0.2, 2 and 10 msec). In contrast, in Ca^{2+}-inhibited channels, long closures (around 2 and 10 msec) became more frequent and openings were dominated by the brief events (0.2 msec). It is clear that the probabilities of specific open and closed durations from each of the cardiac and skeletal RyRs follow very similar trends. This trend is very different from that followed by cardiac RyRs in the activating range of μM [Ca^{2+}] (crosses, Fig. 12). The data in Fig. 12 show that the changes in gating patterns associated with Ca^{2+}-inhibition are the same in cardiac and skeletal RyRs and differ from the changes in gating patterns associated with Ca^{2+}-activation.

Analysis of Probability Distributions of Event Durations

The RyR gating pattern is described by the probability distributions of open and closed durations. Hence we compared the gating mechanisms of skeletal and cardiac RyRs with different Ca^{2+}-sensitivities by comparing their probability distributions.

For a given *cis* [Ca^{2+}], the gating kinetics of cardiac RyRs with different Ca^{2+}-sensitivities differ, partly as a result of variations in the degree of Ca^{2+}-binding to the channels' inhibition site (or sites). In order to dissociate the effects of different Ca^{2+}-binding affinities from the effects of different gating mechanisms, RyRs with similar P_o were compared. For example, if channels with a tenfold difference in Ca^{2+}-sensitivity are compared then the gating of one channel at, for instance, 1 mM Ca^{2+} would be compared with that for the other at 10 mM Ca^{2+}. Such a comparison is made in Fig. 11.

Comparing gating kinetics based on their associated P_o can only apply to a very limited data set because,

Table. Correlation coefficients from paired combinations of experiments on cardiac and skeletal RyRs

C2	C3	C4	C5	C6	C7	C8	S1	S2	S3	S4	Exp #, K_I (mM), n		
0.987	0.961	0.957	0.969	0.924	0.969	0.784	0.963	0.974	0.898	0.953	C1,	1,	3
	0.916	0.955	0.938	0.91	0.982	0.889	0.989	0.982	0.892	0.929	C2,	1,	1
		0.969	0.965	0.939	0.954	0.879	0.976	0.959	0.908	0.988	C3,	5,	4
			0.962	0.962	0.983	0.876	0.982	0.976	0.932	0.961	C4,	7,	6
				0.912	0.985	0.833	0.966	0.958	0.881	0.912	C5,	15,	3
					0.921	0.915	0.886	0.937	0.979	0.941	C6,	22,	1
						0.895	0.991	0.955	0.892	0.926	C7,	–,	1
							0.904	0.919	0.849	0.838	C8,	–,	1
								0.987	0.914	0.934	S1	–,	5
									0.911	0.935	S2	–,	4
										0.919	S3	–,	1
											S4	–,	1

Shown here are correlation coefficients indicating the similarity in the duration-probability distributions obtained from 8 experiments on cardiac RyRs with different [Ca^{2+}] binding affinities (K_I mM; experiments C1–C8) and 4 experiments on skeletal RyRs (S1–S4). Each experiment produced a number (n) of open and closed duration distributions over a range of *cis*[Ca^{2+}]. Each Table entry compares the results from the experiments named in the column and row headings. The top left quadrant of the Table compares experimental results from different cardiac RyRs and the top right quadrant compares all the cardiac and skeletal RyRs. Correlation coefficients in excess of 0.95 indicate close similarity. For example, the data in Fig. 11 produce a correlation coefficient of 0.972.

unlike *cis* [Ca^{2+}] which is known, P_o obtained from each experiment is a variable property of the channel. This problem was overcome by adjusting the probability distributions for small differences in their P_o value as follows:

The probability distributions of open and closed durations (e.g., Fig. 11) are represented by the terms $p_j^o(t_i,P_{oj})$ and $p_j^c(t_i,P_{oj})$ respectively where t_i is the event duration associated with the *ith* sampling bin of the open and closed probability distributions from the *jth* record. The channel open probability, P_{oj}, associated with each probability distribution open and closed times is calculated using Eq. 2

$$P_{oj}=\frac{\sum_i p_j^o(t_i)t_i}{\sum_i p_j^c(t_i)t_i+\sum_i p_j^o(t_i)t_i} \tag{2}$$

The dependence of the probability distributions of closed times on P_o was established by fitting a set of quadratic functions, $Q_i(P_o)$, by least-squares, to the data sets $-\{p_j^c(t_i,P_{oj})\}$ (three such data sets are shown in Fig. 12). Using these functions, the probabilities of specific closed durations from a RyR with an open probability of P_{oj} can be adjusted for a new P_o, namely P_{os}, according to Eq. 3.

$$p_s^c(t_i,P_{os})=p_j^c(t_i,P_{oj})-Q_i(P_{oj})+Q_i(P_{os}) \tag{3}$$

The same method is used to adjust open duration probability distributions for differences in P_o.

The measure of similarity between the gating kinetics of pairs of RyRs is the correlation coefficient which is given by Eq. 4.

$$C=\frac{\frac{1}{n}\sum_{k=1}^{n}(P_k-\bar{P}_k)(S_k-\bar{S}_k)}{\sigma_p\sigma_s} \tag{4}$$

where P_k is the set of data comprising the probabilities of open and closed durations from several recordings of one RyR with different P_o, (i.e., various *cis* [Ca^{2+}]). S_k is the corresponding data set from another RyR which has been adjusted to match the P_o values of P_k. $\bar{P}$, $\bar{S}$, σ_p and σ_s are the means and standard deviations of the data sets P_k and S_k.

Comparison of Cardiac RyRs

The correlation coefficient for all the data shown in Fig. 11*A–D* was 0.972 (1.00 is a perfect match). Correlation coefficients obtained from 28 paired combinations of experiments on cardiac RyRs are given in the Table. Nearly half the paired experiments had correlation coefficients in excess of 0.96. Low correlation coefficients appeared to arise from variations in channel gating that were not associated with Ca^{2+}-inhibition. Finally, we found that pairs of RyRs with similar gating kinetics at sub-inhibiting *cis* [Ca^{2+}] also had similar gating kinetics at higher *cis* [Ca^{2+}]

Comparison of Skeletal and Cardiac RyRs

Probability distributions of open and closed durations from cardiac and skeletal RyRs were also compared ac-

cording to their associated values of P_o. Probability distributions of event durations from 4 skeletal RyRs are compared with those from 8 cardiac RyRs in Fig. 12. The correlation coefficients listed in the Table show that a significant fraction of pairwise comparisons between these channel types have correlation coefficients in excess of 0.96.

The nonparametric analysis used here could not be used to derive a quantitative probability that the gating mechanism in two channel types were the same. If the channel gating is considered to be a Markov process, it is clearly unlikely that different gating mechanisms would give the same $[Ca^{2+}]$-dependent gating pattern. A Markov gating mechanism would require at least 10 "parameters," corresponding to the number of parameters needed to describe the probability distributions (5 for open time distributions and 5 for closed time distributions[2]). Identical gating patterns, over a range of *cis* $[Ca^{2+}]$, would indicate the detailed equivalence of 10 parameters. Such a coincidence arising from two physically distinct gating mechanisms is unlikely. This argument is supported by the observation that the gating patterns of RyR at activating (μM *cis* $[Ca^{2+}]$ and inhibiting $[Ca^{2+}]$ differ (Fig. 12). The probability distributions from four RyRs in activating $[Ca^{2+}]$ correlated poorly with RyRs at inhibiting $[Ca^{2+}]$ (correlation coefficients ranged from −0.2 to 0.8). The different gating patterns reflect the distinct gating mechanisms which are believed to operate for Ca^{2+}-activation and Ca^{2+}-inhibition.

Discussion

The major finding of this work was that cardiac RyRs do exhibit Ca^{2+}-inhibition after incorporation into lipid bilayers. Ca^{2+}-regulation of cardiac RyRs was similar to that reported for SR vesicles and their sensitivity to Ca^{2+} was, on average, 20 times lower than that for skeletal RyRs. Furthermore, the results resolve the previously inconsistent observation that Ca^{2+} inhibits CICR from SR vesicles, but not RyR channels in bilayers (Chu et al., 1993). The RyRs that we studied were functionally normal since a variety of ligands produced typical changes in voltage-dependent ion permeation and gating kinetics (*see* Results).

Variable Gating Kinetics of RyR Channels

A notable feature of the RyR kinetics was their variability which produced a large scatter in our data. However, the relatively modest standard errors (e.g., Fig. 7*A*) are similar in magnitude to those reported elsewhere (e.g., Chu et al., 1993; Shomer et al., 1993). Large variations in gating kinetics are not without precedent. Zahradnikova & Palade (1993) document both bursting and random gating modes for cardiac RyRs. Sitsapesan and Williams (1994) found that the Ca^{2+}-activation characteristics of sheep cardiac RyR exhibited twofold variations in Hill coefficient and fourfold variations Ca^{2+}-sensitivity. Patch clamp and bilayer studies of Ca^{2+}-activation of maxi-K channels (Moczydlowski & Latorre, 1983; Moczydlowski et al., 1985; Laver & Walker, 1991) show 10-fold variations between channels in the $[Ca^{2+}]$ at half activation.

The cause of the variations within each vesicle preparation is not clear. Some possibilities are that (i) there are several RyR isoforms in sheep ventricle, as in avian (Airey et al., 1990) and amphibian skeletal muscle (Murayama & Ogawa, 1992); (ii) RyRs are partially degraded by endogenous calpain II (Rardon et al., 1990); (iii) RyR proteins have different oxidation or phosphorylation states (Witcher et al., 1991); Herrmann-Frank & Varsanyi, 1993); (iv) regulatory proteins, e.g., calmodulin, FK-506 binding protein etc., may be removed from some RyRs (*see below*); (v) technical artefacts are introduced into the experiment. For example, altered channel gating may arise from solvent microlenses or lipid phase separations in the bilayer (White & Thompson, 1973; Fettiplace et al., 1975). Variations in [PS] in the bilayer can modulate the Ca^{2+}-sensitivity of maxi-K channels at low ionic strength (Moczydlowski et al., 1985). However, we found that removal of PS from the lipid did not affect Ca^{2+}-inhibition of RyRs in high ionic strength conditions.

Dissociation of FK-506 binding protein by FK506 has been shown to reduce the inhibitory effect of Ca^{2+} on the open probability skeletal RyRs (Ahern et al., 1994). It is unlikely that FK-506 binding protein is responsible for the variation in Ca^{2+}-inhibition observed in this study because variations in the Ca^{2+}-dependent gating of both skeletal and cardiac RyRs are very different to that induced by the FK-506 binding protein. Dissociation of the FK-506 binding protein from the skeletal RyR increases P_o of RyRs by stabilizing a conductance substate, akin to the effect of ryanodine. Variations in Ca^{2+}-dependence of P_o seem to arise from variations in Ca^{2+}-binding affinity and do not involve substates.

Ca^{2+}-inhibition of the Cardiac RyR in Lipid Bilayers: Why Hasn't It Been Detected Before?

The absence of Ca^{2+}-inhibition from RyRs in other bilayer studies was not due to the range of $[Ca^{2+}]$ tested. Although we use unphysiologically (ludicrously) high cytosolic $[Ca^{2+}]$ (up to 40 mM), 40% of cardiac RyRs showed inhibition with less than 10 mM Ca^{2+}; concentrations used previously (Chu et al., 1993). Similarly, the different results are unlikely to depend on the use of canine or sheep hearts. There are no species differences in Ca^{2+}-inhibition between skeletal RyRs in mammals

[2] The three exponentials which describe the open and closed frequency distributions require six parameters. However, normalizing the data to produce probability distributions reduced the number of independent parameters to five.

(Chu et al., 1993), and no reported species differences in the cardiac isoform. The Ca^{2+}-inhibition of sheep cardiac RyRs was very like that for CICR from canine SR (Chu et al., 1993). Finally, Chu et al., (1993) demonstrated that differences between bilayer and vesicles studies need not arise from procedural differences in different laboratories.

The ready disruption of Ca^{2+}-inhibition by high $[Cs^+]$ (with retention of other ligand responses), provides an explanation for previous differences between SR vesicles and RyRs in bilayers. The composition of the bathing solution could account for the different Ca^{2+}-inhibition properties. CICR was measured with 100 mM K^+ (which does not remove Ca^{2+}-inhibition of cardiac RyRs), whereas bilayer studies were performed with 250 mM Cs^+ (Chu et al., 1993) and high $[Cs^+]$ does remove Ca^{2+}-inhibition. Although Ca^{2+}-inhibition was retained in our sheep cardiac RyRs in 250 mM Cs^+, RyRs from canine hearts may be more sensitive to $[Cs^+]$. Ca^{2+}-inhibition was more robust in skeletal RyRs than in cardiac RyRs. Therefore the different solutions used in CICR and bilayer studies might not affect Ca^{2+}-inhibition in the skeletal RyR.

Ca^{2+}-inhibition in cardiac RyRs: The Ca^{2+}-binding mechanism

The effect of ligands on channel activity is usually considered in two parts: (i) ligand binding, together with the transmission of this event to the channels' ion-gate and (ii) the modification of channel gating induced by the bound ligand. Clues to the nature of the Ca^{2+}-binding mechanism underlying Ca^{2+}-inhibition come from the voltage-dependence of P_o, the variability in K_I and the effects of CHAPS and Cs^+ on inhibition.

The voltage-dependence of P_o (Fig. 4) suggests that the Ca^{2+}-binding site is not close enough to the bilayer to sense the electric field across the membrane. Negative bilayer potentials would reduce the inhibiting effect of cations in the *cis* bath if the cation binding site could sense the electric field (Woodhull, 1973). Therefore the voltage-dependence of the Ca^{2+}-inhibited channel cannot be attributed to voltage-dependent binding of Ca^{2+}.

The Ca^{2+}-inhibition mechanism was disrupted by 500 mM *cis* Cs^+ and must, therefore, be exposed to the cytosolic solution. The permanent loss of Ca^{2+}-inhibition with CHAPS and 500 mM *cis* Cs^+ indicates an irreversible change in the protein, at either the Ca^{2+}-binding site or the link between Ca^{2+}-binding and channel gating. CHAPS has less effect on RyR function than another detergent, digitonin which disrupts a wide range of RyR-ligand interactions (Imagawa et al., 1987). Although high ionic strength buffers are used to dissociate weakly bound membrane proteins, the specificity of Ca^{2+}—inhibition for high $[Cs^+]$ implies that ionic strength is not the only factor involved. Cs^+ is a chaotropic ion which can destabilize protein structure by altering protein-water interactions (Collins & Washabaugh, 1985). Ca^{2+}-inhibition may be disrupted because of a Cs^+-induced dissociation of a cofactor or a conformational change in the RyR. However, the possibility that a portion of the RyR, cleaved off during isolation, is released from the RyR by CHAPS or 500 mM Cs^+ treatments cannot be ruled out. Proteolysis of RyRs with calpain can alter Ca^{2+}-inhibition, while leaving other regulation mechanisms intact (Rardon et al., 1990). It is unlikely that endogenous proteases, released by 500 mM Cs^+, degraded the RyR, since the protein was either exposed to high $[Cs^+]$ on addition of vesicles to the bath, or after fusion with the bilayer. Therefore, the RyRs would be only briefly subjected to proteolysis, and the concentration of enzymes released by Cs^+ would be very low, since the initial protein concentration in the bath was only 10 μg/ml.

The distribution of Ca^{2+}-sensitivities, and the gradual loss of Ca^{2+}-inhibition in high $[Cs^+]$, are *inconsistent* with Ca^{2+}-sensitivity being regulated by a single cofactor. The frequency distribution of Ca^{2+}-sensitivities is unimodal, not the bimodal distribution expected for two channel populations (RyR either bound or unbound to a cofactor). In addition, there was a gradual rise in channel activity with removal of Ca^{2+}-inhibition in 500 mM Cs^+, not the abrupt change expected from the rapid dissociation of a cofactor. A multiplicity of cofactors would not be surprising since the RyR is a homotetrameric protein which could readily bind four cofactor molecules (one per protein subunit).

Comparison of Ca^{2+}-Binding Mechanisms in Skeletal and Cardiac RyRs

The Ca^{2+}-binding properties in cardiac and skeletal RyRs differ in several ways. There was an order of magnitude difference in Ca^{2+}-binding affinities. Ca^{2+}-inhibition in skeletal RyRs was more stable than in cardiac RyRs since 500 mM Cs^+ affected only the cardiac RyR. However, Ca^{2+}-inhibition had the same Hill coefficient ($H = 2$), suggesting that similar reaction schemes could describe Ca^{2+}-binding in both channel types. The molecular basis for the differences in Ca^{2+}-inhibition in cardiac and skeletal RyRs is yet to be determined. Chu et al. (1993) suggests that Ca^{2+}-inhibition in skeletal muscle may be associated with an integral part of the RyR protein, whereas Ca^{2+}-inhibition in cardiac muscle may depend on a more labile inhibition mechanism, possibly involving a peripherally bound protein.

Ca^{2+}-inhibition in Cardiac and Skeletal RyRs: The Ca^{2+}-Gating Mechanism

We considered the possibility that the wide range in Ca^{2+} sensitivity of Ca^{2+}-inhibition was associated with differ-

ences in gating mechanisms. The signature of a channel gating mechanism is the gating pattern it generates which was represented by probability distributions of open and closed durations (Fig. 11). Activation of RyRs by ATP, caffeine and μM Ca^{2+}, and inhibition by high [Ca^{2+}], have distinct effects on channel gating (Fig. 12 and Smith, Coronado & Meissner, 1986; Sitsapesan & Williams, 1990).

The analysis of probability distributions of open and closed durations show that one kinetic model could describe Ca^{2+}-inhibition in cardiac RyRs with high and low Ca^{2+}-sensitivity and Ca^{2+}-inhibition in cardiac and skeletal RyRs. The most likely interpretation of this finding is that the same gating mechanisms operate in these channels. The 20-fold difference in the [Ca^{2+}]-dependence of inhibition in cardiac and skeletal RyRs must be due to different Ca^{2+}-binding mechanisms. This conclusion is consistent with the known RyR sequences. The putative membrane spanning regions of cardiac and skeletal RyR, which presumably includes the peptide sequences responsible for channel gating, have a high degree of identity (Otsu et al., 1990). However, the amino acid sequences which contain putative Ca^{2+}-binding sites (residues 4253 to 4499 in the skeletal RyR; Chen et al., 1992) show little identity between the two channel types (Otsu et al., 1990).

Conclusion

Contrary to previous studies, cardiac RyRs in lipid bilayers exhibited Ca^{2+}-inhibition. The Ca^{2+}-sensitivity of inhibition varied between channels, but on average, was 20-fold less in cardiac RyRs than in skeletal RyRs. The Ca^{2+}-sensitivity of channel inhibition was consistent with [^{3}H]-ryanodine binding to SR vesicles. Ca^{2+}-inhibition was the most fragile property of cardiac RyR, being the only channel property to be disrupted by 500 mM *cis*-Cs^+ and solublization with CHAPS. It is likely that Ca^{2+}-inhibition may not have been observed previously in bilayers because the bathing solutions contained Cs^+. Ca^{2+}-inhibition in skeletal RyRs was more robust than in cardiac RyR and was unaffected by 500 mM Cs^+.

The open and closed probability distributions from different RyRs suggested that the same gating mechanism mediates Ca^{2+}-inhibition in both cardiac and skeletal RyRs and cardiac RyRs with different Ca^{2+}-sensitivities. Differences in Ca^{2+}-inhibition between these channel types depends on differences in their Ca^{2+}-binding properties.

The authors wish to thank Heather Domaschenz for assisting with the experiments and P.W. Gage for his critical assessment of the manuscript. The research was supported by an Australian Research Council Senior Research Fellowship and a grant from the National Heart Foundation.

References

Ahern, G.P., Junankar, P.R., Dulhunty, A.F. 1994. Single channel activity of the ryanodine receptor calcium release channel is modulated by FK-506. *FEBS Lett.* **352:**194–197

Airey, J.A., Beck, C.F., Murakami, K., Tanksley, S.J., Deerinck, T.J., Ellisman, M.H., Sutko, J.L. 1990. Identification and localization of two triad junctional foot protein isoforms in mature avian fast twitch skeletal muscle. *J. Biol. Chem.* **265:**14187–14194

Ashley, C.C., Mulligan, I.P., Lea, T.J. 1991. Ca^{2+} and activation mechanisms in skeletal muscle. *Q. Rev. Biophys.* **24:**1–73

Ashley, R.H., Williams, A.J. 1990. Divalent cation activation and inhibition of single calcium release channels from sheep cardiac sarcoplasmic reticulum. *J. Gen. Physiol.* **95:**981–1005

Brandt, N.R., Caswell, A.H., Wen, S.R., Talvenheimo, J.A. 1990. Molecular interactions of the junctional foot protein and dihydropyridine receptor in skeletal muscle triads. *J. Membrane Biol.* **113:**237–251

Caswell, A.H., Brandt, N.R., Brunschwig, J.P., Purkerson, S. 1991. Localization and partial characterization of the oligomeric disulfide-linked molecular weight 95,000 protein (triadin) which binds the ryanodine and dihydropyridine receptors in skeletal muscle triadic vesicles. *Biochemistry* **30:**7507–7513

Chamberlain, B.K., Volpe, P., Fleischer, S. 1984. Calcium-induced calcium release from purified cardiac sarcoplasmic reticulum vesicles. General characteristics. *J. Biol. Chem.* **259:**7540–7546

Chen, S.R., Zhang, L., MacLennan, D.H. 1992. Characterization of a Ca^{2+} binding and regulatory site in the Ca^{2+} release channel (ryanodine receptor) of rabbit skeletal muscle sarcoplasmic reticulum. *J. Biol. Chem.* **267:**23318–23326

Chu, A., Dixon, M.C., Saito, A., Seiler, S., Fleischer, S. 1988. Isolation of sarcoplasmic reticulum fractions referable to longitudinal tubules and junctional terminal cisternae from rabbit skeletal muscle. *Methods Enzymol.* **157:**36-46

Chu, A., Fill, M., Stefani, E., Entman, M.L. 1993. Cytoplasmic Ca^{2+} does not inhibit the cardiac muscle sarcoplasmic reticulum ryanodine receptor Ca^{2+} channel, although Ca^{2+}-induced Ca^{2+} inactivation of Ca^{2+} release is observed in native vesicles. *J. Membrane Biol.* **135:**49–59

Chung, S.H., Moore, J.B., Xia, L.G., Premkumar, L.S., Gage, P.W. 1990. Characterization of single channel currents using digital signal processing techniques based on Hidden Markov Models. *Philos. Trans. R. Soc. Lond. Biol.* **329:**265–285

Collins, K.D., Washabaugh, M.W. 1985. The Hofmeister effect and the behavior of water at interfaces. *Q. Rev. Biophys.* **18:**323–422

Fabiato, A. 1985. Time and calcium dependence of activation and inactivation of calcium-induced release of calcium from the sarcoplasmic reticulum of a skinned canine cardiac Purkinje cell. *J. Gen. Physiol.* **85:**247–289

Fettiplace, R., Gordon, L.G.M., Hladky, S.B., Requena, J., Zingsheim, H.P., Haydon, D.A., Methods of Membrane Biol. *In: Methods of Membrane Biol,* E.D. Korn, editor. pp. 1–75. Plenum Press, New York 1975,

Fruen, B.R., Mickelson, J.R., Shomer, N.H., Roghair, T.J., Louis, C.F. 1994. Regulation of the sarcoplasmic reticulum ryanodine receptor by inorganic phosphate. *J. Biol. Chem.* **269:**192–198

Herrmann-Frank, A., Varsanyi, M. 1993. Enhancement of Ca^{2+} release channel activity by phosphorylation of the skeletal muscle ryanodine receptor. *FEBS Lett.* **332:**237–242

Ikemoto, N., Ronjat, M., Meszaros, L.G., Koshita, M. 1989. Postulated role of calsequestrin in the regulation of calcium release from sarcoplasmic reticulum. *Biochemistry* **28:**6764–6771

Imagawa, T., Smith, J.S., Coronado, R., Campbell, K.P. 1987. Purified ryanodine receptor from skeletal muscle sarcoplasmic reticulum is

the Ca^{2+}-permeable pore of the calcium release channel. *J. Biol. Chem.* **262:**16636–16643

Jayaraman, T., Brillantes, A.M., Timerman, A.P., Fleischer, S., Erdjument-Bromage, H., Tempst, P., Marks, A.R. 1992. FK-506 binding protein associated with the calcium release channel (ryanodine receptor). *J. Biol. Chem.* **267:**9474–9477

Lai, F.A., Anderson, K., Rousseau, E., Lui, Q.Y, Meissner, G. 1988. Evidence for a Ca^{2+} channel within the ryanodine receptor complex from cardiac sarcoplasmic reticulum. *Biochem. Biophys. Res. Commun.* **151:**441–449

Laver, D.R., Walker, N.A. 1991. Activation by Ca^{2+} and block by divalent ions of the K^+ channel in the membrane of cytoplasmic drops from Chara australis. *J. Membrane Biol.* **120:**131–139

Lindsay, A.R., Williams, A.J. 1991. Functional characterisation of the ryanodine receptor purified from sheep cardiac muscle sarcoplasmic reticulum. *Biochim. Biophys. Acta* **1064:**89–102

Lindsay, A.R., Manning, S.D., Williams, A.J. 1991. Monovalent cation conductance in the ryanodine receptor-channel of sheep cardiac muscle sarcoplasmic reticulum *J. Physiol. Lond.* **439:**463–480

Ma., J. 1995. Desensitization of the skeletal muscle ryanodine receptor: Evidence of hetergeneity of calcium release channels. *Biophys. J.* **68:**893–899

Marty, I., Robert, M., Villaz, M., De Jongh, K.S., Lai, Y., Catterall, W.A., Ronjat, M. 1994. Biochemical evidence for a complex involving dihydropyridine receptor and ryanodine receptor in triad junctions of skeletal muscle. *Proc. Natl. Acad. Sci. USA* **91:**2270–2274

Meissner, G. 1986. Ryanodine activation and inhibition of the Ca^{2+} release channel of sarcoplasmic reticulum. *J. Biol. Chem.* **261:**6300–6306

Menegazzi, P., Larini, F., Treves, S., Guerrini, R., Quadroni, M., Zorzato, F. 1994. Identification and characterization of three calmodulin binding sites of the skeletal muscle ryanodine receptor. *Biochemistry* **33:**9078–9084

Miller, C., Racker, E. 1976. Ca^{++}-induced fusion of fragmented sarcoplasmic reticulum with artificial planar bilayers. *Cell* **9:**283–300

Moczydlowski, E., Alvarez, O., Vergara, C., Latorre, R. 1985. Effect of phospholipid surface charge on the conductance and gating of a Ca^{2+}-activated K^+ channel in planar lipid bilayers. *J. Membrane Biol.* **83:**273–282

Moczydlowski, E., Latorre, R. 1983. Gating kinetics of Ca^{2+}-activated K^+ channels from rat muscle incorporated into planar lipid bilayers. Evidence for two voltage-dependent Ca^{2+} binding reactions. *J. Gen. Physiol.* **82:**511–542

Mueller, P., Rudin, D.O., Tien, H.T., Westcott, W.C. 1962. Reconstitution of cell membrane structure in vitro and its transformation into an excitable system. *Nature* **194:**979–981

Murayama, T., Ogawa, Y. 1992. Purification and characterization of two ryanodine-binding protein isoforms from sarcoplasmic reticulum of bullfrog skeletal muscle. *J. Biochem. Tokyo.* **112:**514–522

Nabauer, M., Callewaert, G., Cleemann, L., Morad, M. 1989. Regulation of calcium release is gated by calcium current, not gating charge, in cardiac myocytes. *Science* **244:**800–803

Otsu, K., Willard, H.F., Khanna, V.J., Zorzato, F., Green, N.M., MacLennan, D.H. 1990. Molecular cloning of cDNA encoding the Ca^{++} release channel (Ryanodine receptor) of rabbit cardiac muscle sarcoplasmic reticulum. *J. Biol. Chem.* **265:**13472–13483

Peng, M., Fan, H., Kirley, T.L., Caswell, A.H., Schwartz, A. 1994. Structural diversity of triadin in skeletal muscle and evidence of its existence in heart. *FEBS Lett.* **348:**17–20

Perrin, D.D., Sayce, I.G. 1967. Computer calculation of equilibrium concentrations in mixtures of metal ions and complexing species. *Talanta* **14:**833–842

Pessah, I.N., Waterhouse, A.L., Casida, J.E. 1985. The calcium-ryanodine receptor complex of skeletal and cardiac muscle. *Biochem. Biophys. Res. Commun.* **128:**449–456

Rardon, D.P., Cefali, D.C., Mitchell, R.D., Seiler, S.M., Hathaway, D.R., Jones, L.R. 1990. Digestion of cardiac and skeletal muscle junctional sarcoplasmic reticulum vesicles with calpain II. Effects on the Ca^{2+} release channel. *Circ. Res.* **67:**84–96IS

Rousseau, E. 1989. Single chloride-selective channel from cardiac sarcoplasmic reticulum studied in planar lipid bilayers. *J. Membrane Biol.* **110:**39–47

Rousseau, E., Meissner, G. 1989. Single cardiac sarcoplasmic reticulum Ca^{2+}-release channel: activation by caffeine. *Am. J. Physiol.* **256:**H328–H333

Rousseau, E., Smith, J.S., Henderson, J.S., Meissner, G. 1986. Single channel and $45Ca^{2+}$ flux measurements of the cardiac sarcoplasmic reticulum calcium channel. *Biophys. J.* **50:**1009–1014

Rousseau, E., Smith, J.S., Meissner, G. 1987. Ryanodine modifies conductance and gating behavior of single Ca^{2+} release channel. *Am. J. Physiol.* **253:**C364–C368

Shomer, N.H.; Louis, C.F.; Fill, M.; Litterer, L.A.; Mickelson, J.R. 1993. Reconstitution of abnormalities in the malignant hyperthermia-susceptible pig ryanodine receptor *Am. J. Physiol.* **264:**C125–C135

Sigworth, F.J., Sine, S.M. 1987. Data transformations for improved display and fitting of single-channel dwell time histograms. *Biophys. J.* **52:**1047–1054

Sitsapesan, R., Montgomery, R.A., MacLeod, K.T., Williams, A.J. 1991. Sheep cardiac sarcoplasmic reticulum calcium-release channels: modification of conductance and gating by temperature. *J. Physiol. Lond.* **434:**469–488

Sitsapesan, R., Williams, A.J. 1990. Mechanisms of caffeine activation of single calcium-release channels of sheep cardiac sarcoplasmic reticulum. *J. Physiol. Lond.* **423:**425–439

Sitsapesan, R., Williams, A.J. 1994. Gating of the native and purified cardiac SR Ca^{2+}-release channel with monovalent cations as permeant species. *Biophys. J.* **67:**1484–1494

Smith, J.S., Coronado, R., Meissner, G. 1986. Single channel measurements of the calcium release channel from skeletal muscle sarcoplasmic reticulum. Activation by Ca^{2+} and ATP and modulation by Mg^{2+}. *J. Gen. Physiol.* **88:**573–588

Timerman, A.P., Jayaraman, T., Wiederrecht, G., Onoue, H., Marks, A.R., Fleischer, S. 1994. The ryanodine receptor from canine heart sarcoplasmic reticulum is associated with a novel FK-506 binding protein. *Biochem. Biophys. Res. Commun.* **198:**701–706

Tinker, A., Lindsay, A.R., Williams, A.J. 1992. A model for ionic conduction in the ryanodine receptor channel of sheep cardiac muscle sarcoplasmic reticulum. *J. Gen. Physiol.* **100:**495–517

Tsien, R.Y. 1980. New calcium indicators and buffers with high selectivity against magnesium and protons; Design, synthesis, and properties of prototype structures. *Biochemistry* **19:**2396–2404

White, S.H., Thompson, T.E. 1973. Capacitance, area, and thickness variations in thin lipid films. *Biochim. Biophys. Acta.* **323:**7–22

Witcher, D.R., Kovacs, R.J., Schulman, H., Cefali, D.C., Jones, L.R. 1991. Unique phosphorylation site on the cardiac ryanodine receptor regulates calcium channel activity. *J. Biol. Chem.* **266:**11144–11152

Woodhull, A.M. 1973. Ionic blockage of sodium channels in nerve. *J. Gen. Physiol.* **61:**687–708

Zahradnikova, A., Palade, P. 1993. Procaine effects on single sarcoplasmic reticulum Ca^{2+} release channels. *Biophys. J.* **64:**991–1003

Zimanyi, I., Pessah, I.N. 1991. Comparison of [^{3}H]ryanodine receptors and Ca^{++} release from rat cardiac and rabbit skeletal muscle sarcoplasmic reticulum. *J. Pharmacol. Exp. Ther.* **256:**938–946